Optimization-based Extrapolation for Truncation Correction

Andreas Maier [1] , Bernhard Scholz [1] , and Frank Dennerlein [2]

Abstract—**A general approach to correct for lateral data truncation in cone-beam CT is presented in which the correction is achieved by minimizing a specific objective function in the projection domain. We suggest an efficient objective function and derive, from the general approach, an iterative truncation correction algorithm. This algorithm is initialized with a water-cylinder-model-based fan-beam extrapolation as it is employed in a clinical product. Compared to using the model-based extrapolation alone, our iterative algorithm improves image quality in the artifact regions at the boundaries of the field-of-view, particularly where the water-cylinder assumptions are not fulfilled. In that case, first quantitative evaluations on a clinical data set indicate an improvement in the root mean square error of up to 18 %.**

Keywords-image reconstruction; truncation; extrapolation; optimization

I. INTRODUCTION

The X-ray dose that the patient receives during a CT exam is proportional to the volume that is irradiated during the scan. Several medical applications require only a small volume to be imaged, so that the irradiated area can be highly restricted. Fig. 1 shows a follow-up scan of a cochlear implant. In this case, a scan with a full field of view was performed although only the small area, indicated by the circle, is of diagnostic interest. Hence, a restriction of the X-ray irradiation to only that area would have been possible to significantly reduce radiation dose.

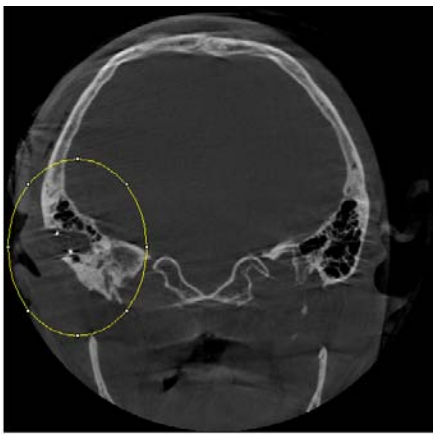

Figure 1: In many diagnostic exams, only a part of the scanned volume is of diagnostic interest. The image shows a follow-up scan of a cochlear implant. The area of interest is marked with an ellipse.

Several practical methods have been suggested for volume-of-interest tomography. Some of them require prior knowledge about the reconstructed object [1] or irradiate parts of the scan at a lower dose [2]. In this paper, however, we will only focus on methods that are able to reconstruct without any other means of prior knowledge.

Reconstruction from laterally severely truncated projection data is an algorithmic challenge. Iterative methods are computationally demanding but might provide solutions if only a part of the object is truncated [3]. In case of bilateral truncation in all views, practically useful results are often obtained by estimating the missing data using heuristic extrapolation methods, e.g. [4]. A good overview on such methods is given in [5]. It is also possible to reconstruct without using any explicit extrapolation scheme [6]. Results are visually satisfying, but generally also approximate.

In this paper, we follow a different approach to solve the truncation problem: We formulate the extrapolation of the missing data as an optimization problem in the projection domain that may involve data before and after filtering. In order to do so, we setup an objective function that describes desired properties of this extrapolation. Then we search for extrapolation values that minimize this objective function using water-cylinder-based fan beam extrapolation values as start values [7]. In the following, we will describe a few properties of truncated and complete filtered projections and will subsequently derive different components of an objective function. Using this objective function, we calculate extrapolation data, and use them for reconstructions and compare their results with reconstruction results from the clinically used extrapolation algorithm using the water-cylinder-based fan beam extrapolation. At the end of this paper, we discuss the properties of the proposed extrapolation algorithm and describe future improvements of the algorithm.

II. EXTRAPOLATION AS OPTIMIZATION PROBLEM

The limited size of the field of measurement can be formulated by a multiplication of the complete row signal $p^*(u,\lambda)$ with a function that describes the size of the field of measurement $d(u,\lambda)$, where $u \in [0, U-1]$ is the index of the detector column, $u_{min}$and u_{max} are the smallest and the highest detector column indices that are still observed, and λ is the current projection angle:

$$d(u,\lambda) = \begin{cases} 1 & u_{min} \le u \le u_{max} \\ 0 & else \end{cases}$$

[1] Siemens AG, Healthcare Sector, Forchheim, ammaier@siemens.com
[2] Siemens AG, Healthcare Sector, Erlangen, frank.dennerlein@siemens.com

The observed row signal $p(u,\lambda)$ is then found as the multiplication of both:

$$p(u,\lambda) = p^*(u,\lambda) \cdot d(u,\lambda)$$

The idea of extrapolation adds new coefficients $x(u)$ to the observed values yielding an extrapolated projection $p'(u,\lambda)$:

$$p'(u,\lambda) = \begin{cases} p(u,\lambda) & u_{min} < u < u_{max} \\ x(u) & else \end{cases}$$

The extrapolated values can be summarized in the vector $\boldsymbol{X}$

$$\boldsymbol{X} = [x(0) \dots x(u_{min}-1)\, x(u_{max}+1) \dots x(U-1)].$$

$\boldsymbol{X}$ is found as the solution to a minimization problem

$$\boldsymbol{X} \leftarrow \operatorname{argmin}_{\boldsymbol{X}} f(\boldsymbol{X}).$$

The challenge to perform an optimal extrapolation is thus the challenge to find an objective function $f(\boldsymbol{X})$ that leads to an extrapolation, which would coincide best with the missing data if they could be measured. In the following, we describe a few properties that are suitable for inclusion in such an objective function.

A. High Frequency Artifact

The predominant artifact that is caused by truncation is a bright ring that is generated at the boundary of the field of view of the reconstructed image. The artifact is caused by the distortion that is introduced into the signal by the convolution of $P^*(\omega,\lambda)$ with $D(\omega,\lambda)$which are the Fourier transforms of $p^*(u,\lambda)$ and $d(u,\lambda)$. The filtered projection data after extrapolation is denoted by $g'(u,\lambda)$ in the following.

The relevant property of the artifact is that it contains high frequencies. We use this to build the following constraint: The signal should only have few high frequency components in Fourier domain. The amount of high frequencies can be described using the 1D frequency representation $G'(\omega,\lambda)$ of $g'(u,\lambda)$

$$c_1 = \sqrt{\sum_{\omega \in \Omega_{high}} G'(\omega,\lambda)^2},$$

where Ω_{high} represents the coefficients of the spectrum that contains the N highest frequencies.

Another relevant property of the filtered projection is that the extrapolated values do not introduce additional signal. This observation is used to design a second term:

$$c_2 = \sqrt{\sum_{u=0}^{U-1} g'(u,\lambda)^2}$$

B. Constant Extrapolation in Reconstruction Domain

As we do not know the object outside the field of measurement, its shape is difficult to describe in a constraint. In most applications, we image objects that are homogenous to some extent. Hence, we can assume that the average absorption coefficient in reconstruction domain at the end of the field of measurement stays in the same range during extrapolation. In order to achieve this constant behavior after backprojection, we also require the filtered projection to be a constant continuation of the known part. Furthermore, we assume that there is only little deviation from this constant continuation. Subtraction of the average value should yield a signal with many zeros, i.e. a sparse signal.

These postulates yield the following constraint:

$$c_3 = \sum_{j=u_{min}-R}^{u_{min}-1} |\overline{g_{min}} - g'(j,\lambda)|_1 + \sum_{j=u_{max}+1}^{u_{max}+R} |\overline{g_{max}} - g'(j,\lambda)|_1$$

with

$$\overline{g_{min}} = \frac{1}{Q} \sum_{j=u_{min}}^{u_{min}+Q-1} g'(j,\lambda)$$

$$\overline{g_{max}} = \frac{1}{Q} \sum_{j=u_{max}-Q+1}^{u_{max}} g'(j,\lambda)$$

where $\overline{g_{min}}$ and $\overline{g_{max}}$ are average values over the left and right end of the filtered projection over an area of Q values and $|\cdot|_1$ describes the L1 norm that promotes sparsity. R denotes the area in which this constant behavior is required.

C. Optimization

Using the criteria defined above, we are now able to define our optimization problem using the following objective function:

$$f(\boldsymbol{X}) = \alpha c_1 + \beta c_2 + \gamma c_3,$$

where α, β, and γ are constants that are used to weigh the influence of each of the constraints.

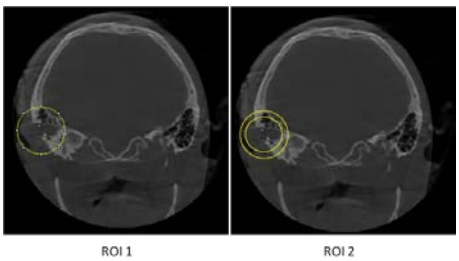

Figure 2: The root mean square error was evaluated over the complete reconstructable area and in an area close to the boundary.

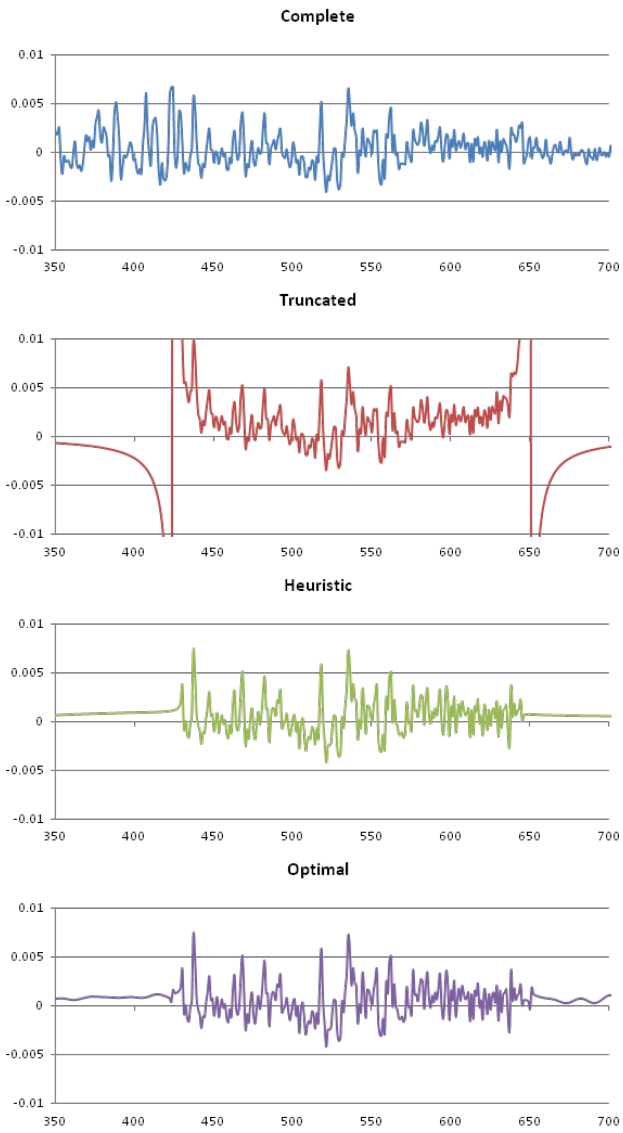

Figure 3: Truncation introduces additional frequencies into the signal that are amplified after filtering. While heuristics can help to reduce this effect, they often suffer from the problem that the remaining signal has a certain slope as seen in the left side of this example. By definition of a constant region at the boundary of the field of view (here R=Q=64), this effect is reduced.

III. Experimental Validation

The scope of this paper is more of an exploratory nature, and to investigate the properties of such a compound objective function. We involve an iterative coordinate-descent for optimization and initialize the iterations using a water-cylinder based fan-beam extrapolation. This model-based extrapolation is also used as a baseline result in the experimental validation.

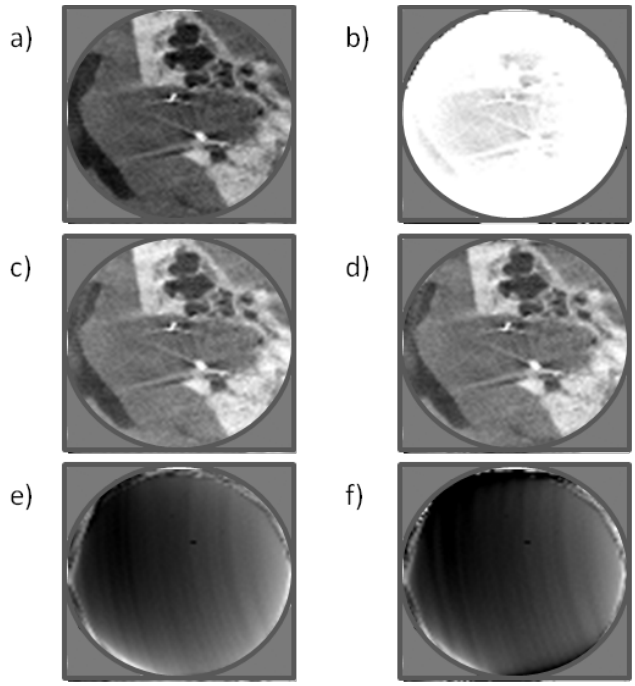

Figure 4: The reconstruction with the complete data is shown in subfigure a). The effect of the truncation is shown in b). Subfigure c) was reconstructed with the heuristic approach. Subfigure d) shows the effect of the optimization ($\alpha = 0.5, \beta = 0.0005$, and $\gamma = 0.4995$). Subfigures e) and f) show the absolute differences between images and a) and c) and a) and d). The darker the image is, the lower the error. The top and the bottom of f) show that the match between a) and d) is improved by the optimization process. The visualization window in Subfigures a-d is [-1000, 2500] HU. In subfigures e) and f) the window is [350, 1000] HU.

In order to speed up the computation, we solved the problems on a multi-resolution grid that started with a very coarse resolution of 64 bins. In each step of the grid search, we increased resolution by a factor of 2 and used the result of the previous iteration as initial value for the optimization problem. In each iteration, we reduced the search space towards the boundary of the field of measurement to speed up computation time further. The optimization parameters were chosen as α=0.5, β=0.0005, γ=0.4995, and $R = Q = 64$.

The reconstruction scenario was the truncated reconstruction of the cochlear implant in Fig.1. The scan was acquired with 496 projections at 1280x960 pixels. Reconstruction was performed at 512^3 voxels with a Shepp-Logan kernel. We chose to evaluate the proposed extrapolation with real data that was truncated artificially. In this manner, we are able to compare the extrapolation result with the reconstruction from the complete signal. The reconstructions are evaluated using the root mean square error (RMSE) on the reconstructable part of the image (ROI 1) and within an area close to the boundary of the field of view (ROI 2, cf. Fig. 2).

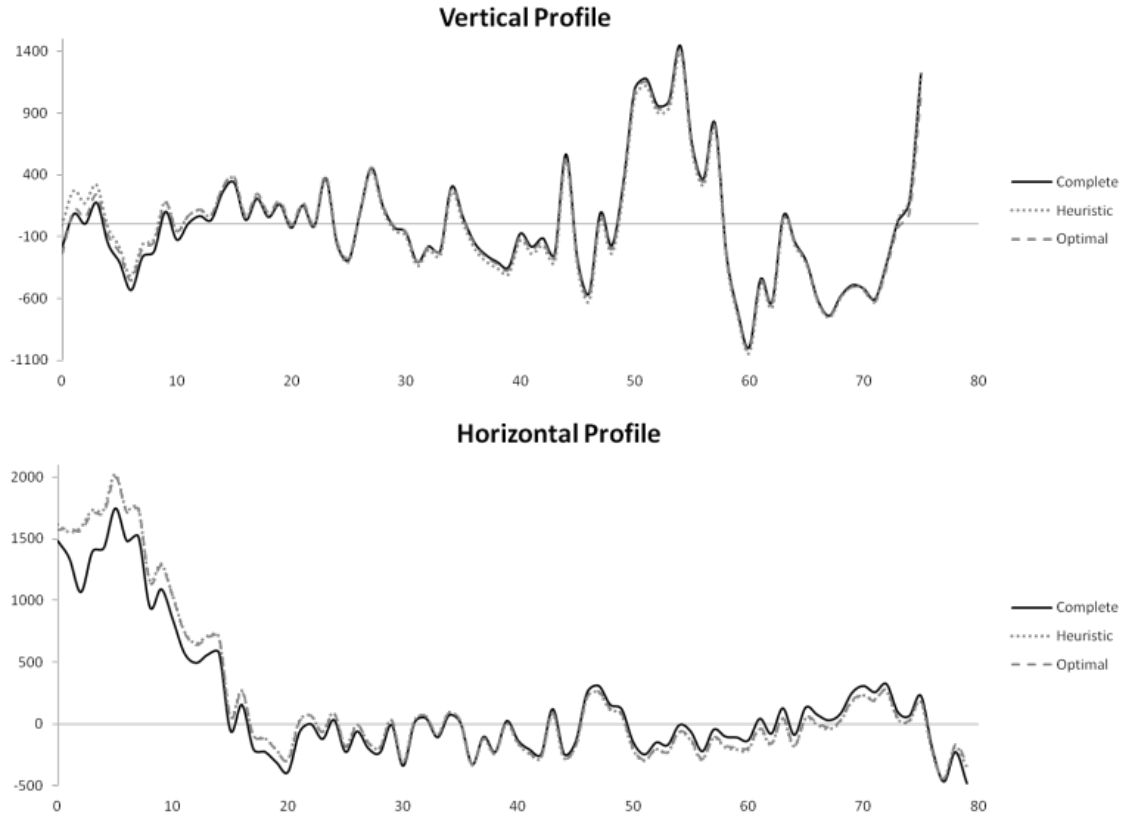

Figure 5: The graphs display two profiles through the reconstructed image. The vertical profile shows an improvement towards the end of the field of measurement. In the horizontal profile no further improvement was obtained compared to the heuristic extrapolation. We subtracted the mean value of each profile to reduce the effect of the offset error.

In Fig. 3 we show the effect of the extrapolation after a Shepp-Logan ramp filter was applied. The optimized signal shows the characteristics that were postulated in the objective function. The signal remains constant in the defined area, has few additional frequencies, and has a low norm.

Fig. 4 shows a comparison between the different reconstructions obtained from the signals from Fig. 4. Subfigure a) shows the reference signal and Subfigure b) the effect of the truncation. In Subfigure c) the reconstruction with the heuristic method is shown. Due to the truncation, the lateral extent of the projection is small, making the fit of a water-cylinder model difficult. The extrapolation is thus degraded and all observed values are increased by an offset. The RMSE for ROI 1 is 557 HU. In ROI 2, the error is even larger with 628 HU. Subfigure d) shows the reconstruction with the optimized extrapolation. Its average RMSE is 500 HU which is lower than in the heuristic extrapolation. At the boundary an average RMSE of 531 HU is obtained. This is only a little higher than the average of the complete ROI, i.e. the reconstruction shows fewer artifacts at the boundary than the heuristic method. The absolute difference images are shown in subfigures e) and f). The error is reduced at the top and the bottom of the image, i.e. in the areas where bones are at the edge of the field of measurement in the projection images. In these areas, the heuristic water cylinder assumption is violated which causes a reduction in image quality. The optimization helps to reduce this artifact.

Fig. 5 shows the effect of the different compensation algorithms on vertical and horizontal profiles through the reconstruction. In order to diminish the offset error, we subtracted the mean values of each of the profiles in the visualization. On the vertical profile, the optimally compensated reconstruction matches the complete reconstruction better. This is especially the case towards the end of the field of measurement. In the horizontal profile, we do not see an improvement compared to the heuristic extrapolation.

IV. Discussion

The results indicate that the presented method is able to improve image quality. The error introduced by the truncation artifact is reduced by 18%. The method seems to be able to yield better extrapolation results in cases where the assumptions of the water cylinder model are not valid. When bone passes through the end of the detector, the heuristic truncation correction algorithm is not able to find a very good solution since the model assumption is invalid. In these cases, the optimization-based method is able to outperform the heuristic method.

In cases that match the water cylinder assumption well, it is difficult to find a better solution with the presented objective function. The optimization-based method then presents the same result as the heuristic method (cf. Fig. 5).

The presented method has an interesting property: As we define parts of the objective function after the filtering step, the optimization is dependent on the used filter kernel. If a smoother kernel is applied, a different extrapolation result is obtained. In the present paper, we employ the method in a Feldkamp-type reconstruction method [8]. In principle, the same method could also be applied to different analytic reconstruction methods that require a completely different filtering step.

The first results indicate that criterion c_2 did not show a lot of importance. A value of $\beta = 0.0005$ was sufficient in our first experiments. The other two criteria were almost balanced with $\alpha = 0.5$ and $\gamma = 0.4995$.

The runtime of the algorithm could be reduced to a feasible amount as we employed multi-grid methods and only applied few iterations (N=5) in the present study. It helped to reduce the search space dramatically, but also limited the solution to one that is rather close to the initial value. This implies that the result of the computation is somewhat dependent on the initialization. At the present state, we decided that the investigation of the objective function was more important than finding an algorithm that is robust of different initializations. We expect this to improve with a more efficient optimization strategy. With respect to the objective function, we could not observe a deterioration that was caused by the method compared to the baseline result.

V. Conclusion and Outlook

We presented a truncation correction method that was inspired by the optimization of an objective function. In a first investigation, we could achieve an improved image quality compared to a water cylinder extrapolation-based algorithm. In an area towards the end of the field of measurement, a reduction of the truncation error of 18 % was obtained. The method could mainly contribute in areas where the water cylinder assumption was violated. This is quite surprising, as only simple assumptions were used in the objective function.

In future work, we will investigate additional constraints that can be used in the objective function. One main concern is that the reconstruction still suffers from an offset error that needs to be reduced. This could be achieved, if the correct size of the object were supplied to the truncation correction method. Improvements of the optimization method are also scope of our current work.

Acknowledgment

The authors wish to thank the Dept. of Neuroradiology, University of Heidelberg, Medical Center, for providing the patient data.

Disclaimer: The concepts and information presented in this paper are based on research and are not commercially available.

References

[1] D. Kolditz, Y. Kyriakou, W.A. Kalender, "Volume-of-interest (VOI) imaging in C-arm flat-detector CT for high image quality at reduced dose," *Med Phys*, vol. 37, no. 6, pp. 2719-2730, 2010.

[2] R. Chityala, K.R. Hoffman, D. R. Bednarek, S. Rudin, "Region of Interest (ROI) Computed Tomograpy," in *Proc. SPIE*, 2004, p. 534.

[3] H. Kunze, W. Härer, K. Stierstorfer, "Iterative extended field of view reconstruction," in *Proc. SPIE*, 2007, p. 6510SX.

[4] Ohnesorge B, Flohr T, Schwarz K, Heiken JP, Bae KT, "Efficient correction for CT image artifacts caused by objects extending outside the scan field of view.," *Med Phys*, vol. 27, no. 1, pp. 39-46, 2000.

[5] G.V. Gompel, *Towards accurate image reconstruction from truncated X-ray CT projections*. Antwerpen, Belgium: University Antwerpen, 2009.

[6] F. Dennerlein, A. Maier, "Region-Of-Interest Reconstruction on medical C-arms with the ATRACT Algorithm," in *Proc. SPIE*, 2012, p. to appear.

[7] B. Scholz, J. Boese, "Correction of Truncation Artifacts in C-Arm CT Images by Fan-Beam Extrapolation Using Savitzky-Golay Filtering," in *RSNA*, 2008, pp. Session SSJ24-06.

[8] A. C. Kak, M. Slaney, *Principles of Computerized Tomographic Imaging*. Piscataway, NJ, United States: IEEE Service Center, 1988.

[9] G. Lauritsch, J. Boese, L. Wigström, H. Kemeth, and R. Fahrig, "Towards cardiac C-arm computed tomography," *IEEE Trans Med Imaging*, vol. 25, pp. 922-34, 2006.

[10] A. Maier, L. Wigström, H. G. Hofmann, J. Hornegger, L. Zhu, N. Strobel, R. Fahrig, "Three-dimensional Anisotropic Adaptive Filter-ing of Projection Data for Noise Reduction in Cone Beam CT," *Med Phys*, vol. 38, no. 11, pp. 5896-5909, 2011.

[11] J. Hsieh, E. Chao. J. Thibault, B. Grekowicz, A. Horst, S. McOlash, "A novel reconstruction algorithm to extend the CT scan field-of-view," *Med Phys*, vol. 31, no. 9, pp. 2385-2391, 2004.